

REPORT DOCUMENTATION PAGE

Form Approved
OMB No. 0704-0188

Public reporting burden for this collection of information is estimated to average 1 hour per response, including the time for reviewing instructions, searching existing data sources, gathering and maintaining the data needed, and completing and reviewing this collection of information. Send comments regarding this burden estimate or any other aspect of this collection of information, including suggestions for reducing this burden to Department of Defense, Washington Headquarters Services, Directorate for Information Operations and Reports (0704-0188), 1215 Jefferson Davis Highway, Suite 1204, Arlington, VA 22202-4302. Respondents should be aware that notwithstanding any other provision of law, no person shall be subject to any penalty for failing to comply with a collection of information if it does not display a currently valid OMB control number. **PLEASE DO NOT RETURN YOUR FORM TO THE ABOVE ADDRESS.**

1. REPORT DATE (DD-MM-YYYY) December 2013		2. REPORT TYPE Technical Paper		3. DATES COVERED (From - To) December 2013- August 2014	
4. TITLE AND SUBTITLE Ab initio Kinetics of Methylamine Radical Thermal Decomposition and H-abstraction From Monomethylhydrazine by H Atom				5a. CONTRACT NUMBER FA9300-06-C-0023	
				5b. GRANT NUMBER	
				5c. PROGRAM ELEMENT NUMBER	
6. AUTHOR(S) H. Sun, G. L. Vaghjiani, C. K. Law,				5d. PROJECT NUMBER	
				5e. TASK NUMBER	
				5f. WORK UNIT NUMBER QORA	
7. PERFORMING ORGANIZATION NAME(S) AND ADDRESS(ES) Air Force Research Laboratory (AFMC) AFRL/RQRP 10 E. Saturn Blvd. Edwards AFB, CA, 93524-7680				8. PERFORMING ORGANIZATION REPORT NO.	
9. SPONSORING / MONITORING AGENCY NAME(S) AND ADDRESS(ES) Air Force Research Laboratory (AFMC) AFRL/RQR 5 Pollux Drive. Edwards AFB, CA, 93524-7048				10. SPONSOR/MONITOR'S ACRONYM(S)	
				11. SPONSOR/MONITOR'S REPORT NUMBER(S) AFRL-RQ-ED-TP-2013-277	
12. DISTRIBUTION / AVAILABILITY STATEMENT Approved for public release; distribution unlimited					
13. SUPPLEMENTARY NOTES Technical Paper presented at 35th Int. Sym. on Combustion; San Francisco, CA, 3-8 Aug, 2014. PA# 14004					
14. ABSTRACT Methylamine radicals (CH ₃ NH) and amino radicals (NH ₂) are the major products in the early ignition/pyrolysis of monomethylhydrazine (CH ₃ NHNH ₂). The kinetics of thermal decomposition of CH ₃ NH radicals was analyzed by RRKM master equation analysis. It was found that β scission of the methyl H atom from CH ₃ NH radicals is dominant and fast enough to induce subsequent H-abstraction reactions to trigger ignition. The gas-phase kinetics of H-abstraction reactions from CH ₃ NHNH ₂ by H atoms was further investigated by <i>ab initio</i> second-order multireference perturbation theory and quadratic-configuration-interaction calculations. It was found that the energy barriers for abstraction of the central amine H atom, two terminal amine H atoms, and methyl H atoms are: 2.95, 4.16, 5.98, and 8.50 kcal mol ⁻¹ , respectively. In units of cm ³ molecule ⁻¹ s ⁻¹ , the corresponding rate coefficients were found to be: $k_7 = 9.63 \times 10^{-20} T^{2.596} \exp(-154.2/T)$; $k_8 = 2.04 \times 10^{-18} T^{2.154} \exp(104.1/T)$; $k_9 = 1.13 \times 10^{-20} T^{2.866} \exp(-416.3/T)$; $k_{10} = 2.41 \times 10^{-23} T^{3.650} \exp(-870.5/T)$, respectively. The results reveal that abstraction of the terminal amine H atom to form trans-CH ₃ NHN•H radicals is the dominant channel among the different abstraction channels. At 298K, the total theoretical H-abstraction rate coefficient, calculated with no adjustable parameters, is 8.16×10^{-13} cm ³ molecule ⁻¹ s ⁻¹ , which is in excellent agreement with the experimental observation of $(7.60 \pm 1.14) \times 10^{-13}$ cm ³ molecule ⁻¹ s ⁻¹ (Vaghjiani, <i>J. Phys. Chem. A</i> , 1997).					
15. SUBJECT TERMS					
16. SECURITY CLASSIFICATION OF:			17. LIMITATION OF ABSTRACT	18. NUMBER OF PAGES	19a. NAME OF RESPONSIBLE PERSON
a. REPORT	b. ABSTRACT	c. THIS PAGE			G. Vaghjiani
Unclassified	Unclassified	Unclassified	SAR	19	19b. TELEPHONE NO (include area code) 661-275-5657

Standard Form
298 (Rev. 8-98)
Prescribed by ANSI
Std. Z39.18

***Ab initio* Kinetics of Methylamine Radical Thermal Decomposition and H-abstraction from Monomethylhydrazine by H Atom**

Hongyan Sun¹, Ghanshyam L. Vaghjiani¹, and Chung K. Law²

¹Air Force Research Laboratory, AFRL/RQRP, Edwards AFB, California 93524, USA

²Department of Mechanical and Aerospace Engineering, Princeton University, Princeton, New Jersey 08544

Abstract

Methylamine radicals (CH₃NH) and amino radicals (NH₂) are the major products in the early ignition/pyrolysis of monomethylhydrazine (CH₃NHNH₂). The kinetics of thermal decomposition of CH₃NH radicals was analyzed by RRKM master equation analysis. It was found that β scission of the methyl H atom from CH₃NH radicals is dominant and fast enough to induce subsequent H-abstraction reactions to trigger ignition. The gas-phase kinetics of H-abstraction reactions from CH₃NHNH₂ by H atoms was further investigated by *ab initio* second-order multireference perturbation theory and quadratic-configuration-interaction calculations. It was found that the energy barriers for abstraction of the central amine H atom, two terminal amine H atoms, and methyl H atoms are: 2.95, 4.16, 5.98, and 8.50 kcal mol⁻¹, respectively. In units of cm³ molecule⁻¹ s⁻¹, the corresponding rate coefficients were found to be: $k_7 = 9.63 \times 10^{-20} T^{2.596} \exp(-154.2/T)$; $k_8 = 2.04 \times 10^{-18} T^{2.154} \exp(104.1/T)$; $k_9 = 1.13 \times 10^{-20} T^{2.866} \exp(-416.3/T)$; $k_{10} = 2.41 \times 10^{-23} T^{3.650} \exp(-870.5/T)$, respectively. The results reveal that abstraction of the terminal amine H atom to form trans-CH₃NHN•H radicals is the dominant channel among the different abstraction channels. At 298K, the total theoretical H-abstraction rate coefficient, calculated with no adjustable parameters, is 8.16×10^{-13} cm³ molecule⁻¹ s⁻¹, which is in excellent agreement with the experimental observation of $(7.60 \pm 1.14) \times 10^{-13}$ cm³ molecule⁻¹ s⁻¹ (Vaghjiani, *J. Phys. Chem. A*, 1997).

Key words: CH₃NH decomposition, CH₃NHNH₂, H-abstraction, CASPT2, rate coefficient

1. Introduction

The binary system of monomethylhydrazine (CH_3NHNH_2) and dinitrogen tetroxide (N_2O_4) is widely used as liquid propellants for satellite and space propulsion applications [1]. It is known that the N—N bond strength is weaker than that of the C—N bond in CH_3NHNH_2 , and as such, the CH_3NH and NH_2 radicals from N—N bond fission are the major products in the early ignition/pyrolysis of CH_3NHNH_2 [2]. Using the high-pressure limit rate coefficients of CH_3NHNH_2 decomposition [3], the branching ratio between the N—N bond fission and C—N bond fission was found to be 95:5 at a temperature of 1000K and for pressures in the range of 2 to 3 atm. To experimentally quantify the pressure-dependent rate coefficients for the N—N bond fission, Hanson's group [4] recently measured the NH_2 concentration time-histories in $\text{CH}_3\text{NHNH}_2/\text{Ar}$ mixtures over the temperature range of 1100 to 1400K and pressures in the range of 0.3 to 5 atm behind reflected shock waves using laser absorption measurement methods. The fate of the CH_3NH radicals however was not reported. Theoretically, we have found that the CH_3NH radical is very reactive since direct β -scission of the methyl H atom in CH_3NH has a small energy barrier to form amino-methylene ($\text{CH}_2=\text{NH}$) as the stable product. Furthermore, the H atoms generated from this decomposition reaction will react with the unburned fuel molecules to induce ignition.

In this work, the kinetics of the thermal decomposition of CH_3NH radicals was analyzed and pressure dependent rate coefficients for the dominant reaction pathways determined by RRKM master equation analysis. Furthermore, the kinetics of H-abstraction from CH_3NHNH_2 by H atoms was analyzed using second-order multireference perturbation theory and unrestricted quadratic-configuration-interaction QCISD(T) calculations. The rate coefficients for each of the abstraction channels were quantified by micro-canonical transition state theory, and the associated branching ratios determined. It was found that the total rate coefficient determined from *ab initio* kinetics theories is in

excellent agreement with the experimental value observed at room temperature [5]. Thus the theoretical rate coefficients from this work should be reliable over a wide temperature range and are essential parameters in the development of reaction mechanisms for the kinetics modeling of ignition involving monomethylhydrazine and its derivatives.

2. Electronic Structures

There are several reaction pathways for the CH_3NH radical decomposition, which include β scission, isomerization, molecular elimination, and bond fission. The geometries of the stationary points of the potential energy surfaces (PESs) for these reactions were optimized at the B3LYP/6-311++G(d,p) level, except for bond fission reactions. For the C—N and N—H bond fission reactions in CH_3NH , multi-reference character of the wave functions is significant. Hence geometries of the transition states for these two bond breaking channels were optimized by multireference second-order perturbation theory [6] with appropriate orbitals included in the active space. The C—N and N—H bond fissions involve doublet and quartet PESs because of the parallel and antiparallel alignment of electron spins in the NH and CH_3N radicals. Since the energy of $\text{NH}(X^3\Sigma^-)$ is 42.73 kcal/mol lower than that of $\text{NH}(a^1\Delta)$, the reaction path leading to the $\text{CH}_3 + \text{NH}(X^3\Sigma^-)$ products is energetically favorable. This is also true in the case for the triplet, $^3\text{CH}_3\text{N}$ product formation. Therefore, the transition state structures in C—N and N—H bond fission reactions were determined for the triplet products formation. Specifically, for the $\text{CH}_3 + \text{NH}(X^3\Sigma^-)$ dissociation channel, the active space includes the bonding orbital between the p orbital of the N atom and the p orbital of the C atom, as well as a perpendicular p orbital for the radical on the NH fragment. Similarly, for the $^3\text{CH}_3\text{N} + \text{H}$ dissociation channel, the active space includes the bonding orbital between the p orbital of the N atom and the s orbital of the H atom, as well as a perpendicular p orbital for the radical on the CH_3N fragment. Such orbital configurations were included

in the active space of the transition state to acquire a parallel alignment of electron spins on the corresponding N atom for the formation of the triplet NH and $^3\text{CH}_3\text{N}$ products.

For the abstraction of amine hydrogen atoms by H atom, the multi-reference character of the wave functions was also found to be quite significant, as reflected by their T1 diagnostics [6] of 0.03 from QCISD(T)/cc-pVQZ calculations. The CASPT2 method with aug-cc-pVDZ and aug-cc-pVTZ basis sets was applied to optimize the geometries of reactants and transition states, and to calculate the ro-vibrational frequencies. In the CASPT2 geometry optimizations, the active space (4e,3o) was chosen for CH_3NHNH_2 , consisting of the σ , σ^* orbital pair of the N—N bond and the s orbital of the amine N atom. The active space (3e,3o) consisting of the H atom orbital and the σ , σ^* orbital pair of the H atom being abstracted was chosen for the transition states for the abstraction of amine H atoms. For abstraction of the methyl H atom, the orbitals of the N—N and C—N bonds become delocalized. Consequently, a larger active space (7e,5o) consisting of the H atom orbital, the σ , σ^* orbital pair of the methyl H atom being abstracted, and the two hybrid orbitals between the methyl and the NH groups was chosen for the transition state for the abstraction of methyl hydrogen.

Higher-level single-point energies were determined from the spin unrestricted or restricted quadratic-configuration-interaction QCISD(T) calculations for open-shell and closed-shell species. The cc-pVTZ and cc-pVQZ basis sets were adopted in the QCISD(T) calculations and the energies were extrapolated to the complete basis set (CBS) limit, cc-pV ∞ Z, by the asymptotic form [7][8]. Electronic structure calculations were performed using the MOLPRO [9] and Gaussian09 [10] program packages.

3. Kinetics of CH_3NH Radical Decomposition

The thermal decomposition of the CH_3NH radicals was found to occur by the following reaction pathways:



DISTRIBUTION A: Approved for public release, distribution unlimited

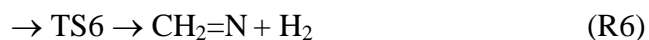
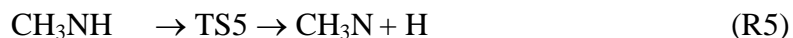


Figure 1 shows the stationary points of the potential energy surfaces of the CH_3NH radical decomposition characterized at the UQCISD(T)//cc-pV ∞ Z level with CASPT2/cc-pVTZ and B3LYP/6-311++G(d,p) geometries. For the C—N bond fission (R1), a saddle point with a doublet state (TS1) was found to have an energy of 79.51 kcal/mol higher than that of the CH_3NH radical, and it is 2.98 kcal/mol higher than that of the $\text{CH}_3 + \text{NH}(X^3\Sigma^-)$ channel. The β scission of the methyl H atom from the CH_3NH radical was found to have an energy barrier of 33.08 kcal/mol, forming amino-methylene ($\text{CH}_2=\text{NH}$) (R2). Isomerization of the CH_3NH radical produces the CH_2NH_2 radical with an energy barrier of 36.39 kcal mol⁻¹ (R3). The CH_2NH_2 radical formed also undergoes β scission of the amine H atom with an energy barrier of 39.37 kcal/mol, forming $\text{CH}_2=\text{NH}$ (R4). The N—H bond fission reaction in the CH_3NH radical that leads to the triplet $^3\text{CH}_3\text{N}$ radical and H atom is endothermic by 83.86 kcal mol⁻¹ (R5). The doublet transition state (TS5) was found to have an energy of 0.54 kcal/mol lower than its products. A direct H_2 elimination from the CH_3NH radical is endothermic by 13.24 kcal mol⁻¹ (R6), but its energy barrier is quite high, 99.62 kcal mol⁻¹, and is not kinetically relevant.

In the decomposition of CH_3NH radicals, micro-canonical rate coefficients as functions of total rotational-vibrational energy (E) and total angular momentum (J) were calculated using Rice–Ramsperger–Kassel–Marcus (RRKM) theory and multi-well master equation analysis [11][12][13] which were implemented in the VARIFLEX code [14]. Tunneling corrections were included for all transition states based on asymmetric Eckart potentials [15]. Pressure-dependent kinetics analysis was

performed by solving the time-dependent, multiple-well master equation. The collisional energy transfer probability in the master equation analysis was approximated by a single-exponential-down model, employing the temperature dependent form, $\Delta E_{down} = 200(T/300)^{0.85} \text{ cm}^{-1}$, for the average downward energy transfer [16]. The Lennard-Jones parameters for the collision rates were estimated to be $\sigma = 3.8 \text{ \AA}$ and $\varepsilon = 253 \text{ cm}^{-1}$ for the CH_3NH radical, and $\sigma = 3.70 \text{ \AA}$ and $\varepsilon = 66.1 \text{ cm}^{-1}$ for nitrogen [17].

We chose $\text{CH}_3 + \text{NH}(X^3\Sigma^-) \rightarrow \text{CH}_3\text{NH}$ (R-1) as an entrance channel to determine the phenomenological rate coefficients. At a pressure of 1 atm, the rate coefficients for three dominant decomposition channels (R2, R3, and R4) were obtained and fitted as the following expressions in the temperature range of 600 to 2500K.

$$k_2 = 2.69 \times 10^{27} \text{ T}^{-4.767} \exp(-18598.9/T) \text{ s}^{-1}$$

$$k_3 = 1.02 \times 10^{30} \text{ T}^{-6.038} \exp(-18823.9/T) \text{ s}^{-1}$$

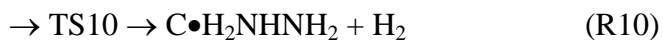
$$k_4 = 1.85 \times 10^{31} \text{ T}^{-5.755} \exp(-22570.3/T) \text{ s}^{-1}$$

It is noted that due to the uncertainties in the parameters for the average energy transfer model, the above pressure dependent rate coefficients need to be further quantified/validated by future experimental measurements. Nevertheless, these rate coefficients should be useful for kinetics analysis for the CH_3NH radical decomposition. Figure 2 shows the rate coefficients k_2 , k_3 , and k_4 at 1 atm along with the corresponding high-pressure limit rate coefficients in the range of 600 - 2500K. It is seen that the direct dissociation rate (k_2) to $\text{CH}_2=\text{NH} + \text{H}$ is dominant at all temperatures. The dissociation rate (k_4) to $\text{CH}_2=\text{NH} + \text{H}$, is comparable to k_2 only when the temperature is above $\sim 1800\text{K}$. The isomerization rate coefficient (k_3) to CH_2NH_2 is about one order of magnitude smaller than k_2 . This is ascribed to the tight three-center transition state (TS3) with an imaginary frequency of 1991.6 cm^{-1} , while the β scission of the methyl H atom occurs via a looser transition state (TS2) with an imaginary frequency of 555.4 cm^{-1} . Furthermore, strong pressure dependence in the dissociation rates is observed, and β scission of the

methyl H atom to form $\text{CH}_2=\text{NH}$ dominates at all pressures. Between 1 atm and the high pressure limit, the rate coefficient k_2 was found to be in the range from 1.6×10^6 to $8.7 \times 10^7 \text{ s}^{-1}$, and is fast enough to produce H atoms that can subsequently abstract H atoms from unburned fuel molecules to trigger ignition. In the following section, the kinetics of H-abstraction from CH_3NHNH_2 by H atoms is analyzed.

4. Kinetics of H-Abstraction from CH_3NHNH_2 by H atom

For the direct abstraction of different H atoms from CH_3NHNH_2 by H atoms, four distinct radicals are possible, as shown in Figure 3.



For the $\text{CH}_3\text{NHN}\bullet\text{H}$ radical, it is noted that the geometry with the terminal amine H atom trans to the methyl group is defined as the trans- $\text{CH}_3\text{NHN}\bullet\text{H}$ radical, and the geometry with the terminal amine H atom cis to the methyl group is defined as the cis- $\text{CH}_3\text{NHN}\bullet\text{H}$ radical. In these CASPT2 optimized transition state geometries, the cleaving N—H bond lengths are 1.137, 1.128, and 1.163 Å, and the forming H—H bond lengths are 1.071, 1.127, and 1.038 Å in TS7, TS8, and TS9, respectively. In TS10, the cleaving C—H bond length is 1.232 Å and the forming H—H bond length is 1.172 Å. In comparing the above cleaving and forming bond length data, it is seen that the formation of the trans- $\text{CH}_3\text{NHN}\bullet\text{H}$ radical via TS8 should be more facile because of the longer forming H—H bond length. This implies a low energy barrier in this channel and as such is the dominant reaction path.

With the optimized geometries in Figure 3, the rotational and vibrational frequencies of the four transition states were calculated at the same CASPT2/cc-pVTZ level. The T1 diagnostics, zero-point energies, and zero-point corrected UQCISD(T)/cc-pV ∞ Z energies relative to that of CH₃NHNH₂ + H channel are listed in Table 1. The four abstraction channels (R7 through R10) have energy barriers of 4.16, 2.95, 5.98, and 8.50 kcal mol⁻¹, respectively. The channels for the abstraction of amine H atoms are exothermic by 23 to 25 kcal mol⁻¹, while the channel for the abstraction of the methyl H atom is less exothermic (11.7 kcal mol⁻¹). The abstraction of a terminal amine H atom to form trans-CH₃NHN•H + H₂ (R8) has the lowest energy barrier of 2.95 kcal mol⁻¹ among the four transition states, which is due to the longer forming H—H bond in TS8 as discussed above. It is expected to be the dominant channel among these abstraction reactions.

The rate coefficients of the above H-abstraction reactions were determined using (*E*, *J*) resolved micro-canonical transition state theory with the CASPT2/aug-cc-pVTZ optimized geometries and vibrational frequencies. Hindered rotor corrections for the C–N and N–N torsional modes were obtained from one-dimensional fits of the torsional potentials, employing Pitzer-Gwinn like approximations [18] and the I^(2,3) moments of inertia that reproduced the coupled-harmonic-oscillator limit at low temperatures, and the free-rotor limit at high temperatures. Tunneling effects through the saddle points were modeled with asymmetric Eckart potentials. The imaginary frequencies of the four transition states used for the tunneling corrections are: 1895.4, 1674.7, 1969.9, and 2151.2 cm⁻¹, respectively, which were obtained from the CASPT2/cc-pVTZ calculations. The calculated rate coefficients for the abstraction of different H atoms in CH₃NHNH₂ by H atom are shown in Figure 4. The rate coefficient *k*₈ for the abstraction of the terminal amine H atom to form trans-CH₃NHN•H + H₂ dominates below 1500K. Furthermore, the rate coefficient *k*₈ is within the lower limit of the reported experimental rate coefficient at 298K [5], which implies that the channel (R8) is the predominant

abstraction channel. Due to the small energy barrier, tunneling effects on k_8 are expected to be significant at low temperatures. The tunneling factor for k_8 was found to be in the range of 6.20 - 1.71 for temperatures in the range of 298 - 600K, and decreases to 1.37 - 1.04 in the higher temperature range of 800 - 2500K. The abstraction of the central amine H atom (R7) becomes dominant above 1500K, whereas reactions (R9) and (R10) become important at temperatures above 1000K. It is seen that the reactions are governed by the abstraction of the amine hydrogen atoms at low temperatures, and the abstraction of the methyl H atoms becomes important at high temperatures. Furthermore, β -scission of NH_2 from the $\text{C}\bullet\text{H}_2\text{NHNH}_2$ radical is the fastest process among the decomposition channels of the four radicals [19]. Therefore all of the abstraction channels are important pathways in the CH_3NHNH_2 pyrolysis/oxidation. In units of $\text{cm}^3 \text{ molecule}^{-1} \text{ s}^{-1}$, the rate coefficients were fitted as follows:

$$k_7 = 9.63 \times 10^{-20} T^{2.596} \exp(-154.2/T)$$

$$k_8 = 2.04 \times 10^{-18} T^{2.154} \exp(104.1/T)$$

$$k_9 = 1.13 \times 10^{-20} T^{2.866} \exp(-416.3/T)$$

$$k_{10} = 2.41 \times 10^{-23} T^{3.650} \exp(-870.5/T)$$

Assuming the rate coefficients are additive, the total rate coefficient k_{total} was determined to be $2.55 \times 10^{-20} T^{2.896} \exp(227.6/T) \text{ cm}^3 \text{ molecule}^{-1} \text{ s}^{-1}$. At room temperature, the theoretical rate coefficient is $8.16 \times 10^{-13} \text{ cm}^3 \text{ molecule}^{-1} \text{ s}^{-1}$, and as seen in Figure 4, it is in the upper bound of the experimental observation of $(7.60 \pm 1.14) \times 10^{-13} \text{ cm}^3 \text{ molecule}^{-1} \text{ s}^{-1}$ [5]. The excellent agreement between theory and experiment for the total rate coefficient at room temperature gives us confidence in the accuracy of the theoretical rate coefficients at high temperatures. Based on these theoretical rate coefficients, the branching ratios as a function of temperatures are plotted in Figure 5. k_8 for forming the $\text{trans-CH}_3\text{NHN}\bullet\text{H}$ radical is shown to be the predominant rate coefficient among all of the abstraction channel

rate coefficients for temperatures below 1200K. This is consistent with our previous study on the related H atom abstraction from CH₃NHNH₂ by OH radicals [20].

Recently, a kinetics analysis on the reactions of CH₃NHNH₂ + H/D was performed by Wang *et al.* [21] based on quantum chemistry calculations at the MCG3-MPWPW91//MPW1K/6-311G(d,p) level, which yielded a value for the total rate coefficient of $1.47 \times 10^{-19} T^{2.74} \exp(-239.1/T)$ cm³ molecule⁻¹ s⁻¹ in the temperature range of 200 to 2000K. Their calculated total rate coefficient at 298K is 4.14×10^{-13} cm³ molecule⁻¹ s⁻¹, which is a factor of 2 lower than the experimental value [5]. The discrepancy in the total rate coefficient value between the study of Wang *et al.* [21] and this work is in the range 2 - 0.7 in the temperature range of 300 - 2500K. In their analysis, Wang *et al.* considered the H-abstraction reactions of two CH₃NHNH₂ isomers with six distinguishable pathways for each isomer. The rate coefficient for each reaction channel was calculated by using canonical variational transition state theory with a small-curvature tunneling correction (CVT/SCT), and all of the rotational and vibrational frequencies were treated by the harmonic-oscillator approximation. The total rate coefficient was determined by summation of the individual rate coefficient contributions from each of the isomers using weighting factors in the Boltzmann distribution function. Furthermore, they concluded that the H atom abstraction from the central NH group is the dominant channel below 500K, which is contrary to our findings. We note here that the branching ratios will certainly affect the radical product distributions when modeling CH₃NHNH₂ pyrolysis and oxidation.

In this work, we have carried out high-level UQCISD(T)/cc-pV ∞ Z//CASPT2/aug-cc-pVTZ calculations to obtain accurate values for the molecular properties and energy values for the species involved in this system. The rate coefficient was computed by micro-canonical transition state theory with conservation of total rotational-vibrational energy (E) and total angular momentum (J), and the torsional anharmonicities were treated as internal rotations for the rotational conformers. Consequently,

our approach should provide a better perspective for the branching ratios as well as absolute values of the temperature dependent rate coefficients.

5. Concluding Remarks

The kinetics of the thermal decomposition of CH_3NH radicals was analyzed and pressure dependent rate coefficients of the dominant reaction pathways were determined by RRKM master equation analysis. β scission of methyl H atom to form the $\text{CH}_2=\text{NH}$ product was found to be the most dominant channel in the CH_3NH radical decomposition. Furthermore, the kinetics of H-abstraction from CH_3NHNH_2 by H atoms was analyzed using second-order multireference perturbation theory and unrestricted quadratic-configuration-interaction QCISD(T) calculations. The rate coefficient for each channel was calculated at the (E, J) resolved level using micro-canonical transition state theory, and the corresponding branching ratios for the product channels determined. The results reveal that the abstraction of the terminal amine H atom to form $\text{trans-CH}_3\text{NHN}\bullet\text{H}$ radical is the most dominant channel among all the abstraction channels. The total theoretical rate coefficient computed is in excellent agreement with the available experimental data.

Acknowledgments

The National Research Council is thanked for the Senior Research Associateship Award to H. Sun at the Air Force Research Laboratory, Edwards AFB under Contract No. FA9550-12-d-0001. This research used resources of the National Energy Research Scientific Computing Center, which is supported by the Office of Science of the U.S. Department of Energy under Contract No. DE-AC02-05CH11231.

References

- [1] E. W. Schmidt, *Hydrazine and its derivatives: preparation, properties, applications* 2nd ed., John Wiley & Sons, Inc., New York, **2001**.

- [2] H. Sun, C. K. Law, *J. Phys. Chem. A* **2007**, *111*, 3748-3760.
- [3] P. Zhang, S. J. Klippenstein, H. Sun, C. K. Law, *Proc. Combust. Inst.* **2011**, *33*, 425-432.
- [4] S. Li, D. F. Davidson, R. K. Hanson, *Combust. Flame* **2014**, *161*, 16-22.
- [5] G. L. Vaghjiani, *J. Phys. Chem. A* **1997**, *101*, 4167-4171.
- [6] H.-J. Werner, P. J. Knowles, *J. Chem. Phys.* **1985**, *82*, 5053-5063.
- [7] J. M. L. Martin, *Chem. Phys. Lett.* **1996**, *259*, 669-678.
- [8] D. Feller, D. A. Dixon, *J. Chem. Phys.* **2001**, *115*, 3484-3495.
- [9] Werner, H.-J.; Knowles, P. J.; Knizia, G.; Manby, F. R.; Schütz, M. and others, MOLPRO, version 2010.1, a package of *ab initio* programs, see <http://www.molpro.net>.
- [10] Frisch, M. J.; Trucks, G. W.; Schlegel, H. B.; Scuseria, G. E.; Robb, M. A.; Cheeseman, J. R.; Scalmani, G.; Barone, V.; Mennucci, B.; Petersson, G. A. et al. Gaussian 09, Revision A.1, Gaussian, Inc., Wallingford CT, 2009.
- [11] J. A. Miller, S. J. Klippenstein, *J. Phys. Chem. A* **2006**, *110*, 10528-10544.
- [12] A. Fernández-Ramos, J. A. Miller, S. J. Klippenstein, D. G. Truhlar, *Chemical Reviews* **2006**, *106*, 4518-4584.
- [13] J. A. Miller, S. J. Klippenstein, *J. Phys. Chem. A* **2003**, *107*, 2680-2692.
- [14] Klippenstein, S. J.; Wagner, A. F.; Dunbar, R. C.; Wardlaw, D. M.; Robertson, S. H.; Miller, J. A.; VARIFLEX: version 2.02m, 2010.
- [15] H. S. Johnston, J. Heicklen, *J. Phys. Chem.* **1962**, *66*, 532-533.
- [16] J. A. Miller, S. J. Klippenstein, *Phys. Chem. Chem. Phys.* **2004**, *6*, 1192-1202.
- [17] J. O. Hirschfelder, C. F. Curtiss, R. B. Bird, *Molecular theory of gases and liquids*, Wiley, New York, **1954**.
- [18] K. S. Pitzer, W. D. Gwinn, *J. Chem. Phys.* **1942**, *10*, 428-440.

- [19] H. Sun, P. Zhang, C. K. Law, *J. Phys. Chem. A* **2012**, *116*, 8419-8430.
- [20] H. Sun, P. Zhang, C. K. Law, *J. Phys. Chem. A* **2012**, *116*, 5045-5056.
- [21] L. Wang, Y. Zhao, J. Wen, J. Zhang, *Theor. Chem. Accounts* **2013**, *132*, 1321.

TABLE1. Molecular Properties for CH₃NHNH₂ + H Reaction

Transition state	T1 diagnostic ^a	ZPE ^b	ΔE ^c	ΔE ^d
TS7_CH ₃ N•NH ₂	0.029	49.76	4.16	4.27
TS8 _trans-CH ₃ NHN•H	0.031	50.13	2.95	3.44
TS9_cis-CH ₃ NHN•H	0.028	49.79	5.98	5.91
TS10_C•H ₂ NHNH ₂	0.018	50.08	8.50	8.11

^a T1 diagnostics calculated at the QCISD(T)/cc-pVQZ level. ^b Zero-point energy calculated at the CASPT2/aug-cc-pVTZ level, units in kcal mol⁻¹. ^c Zero-point corrected energy relative to the reactants CH₃NHNH₂ + H calculated at the QCISD(T)/cc-pV ∞ Z//CASPT2/aug-cc-pVDZ level, units in kcal mol⁻¹. ^d Zero-point corrected energy relative to the reactants CH₃NHNH₂ + H calculated at the MCG3-MPWPW91 //MPW1K/6-311G(d,p) level by Wang et al. [21], units in kcal mol⁻¹.

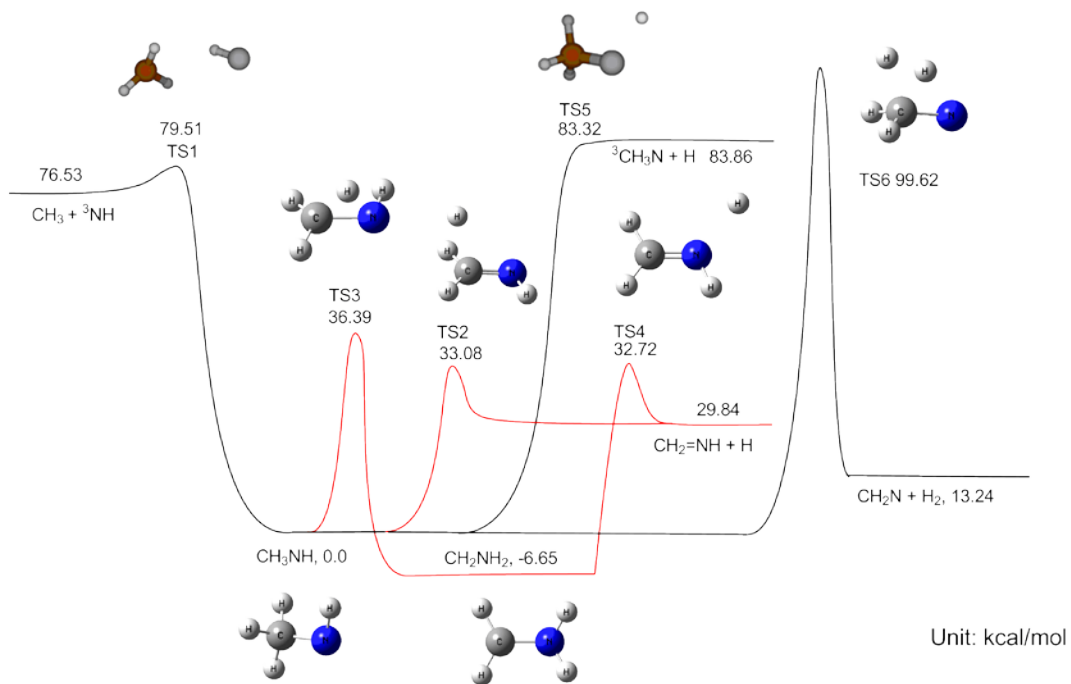


Figure 1

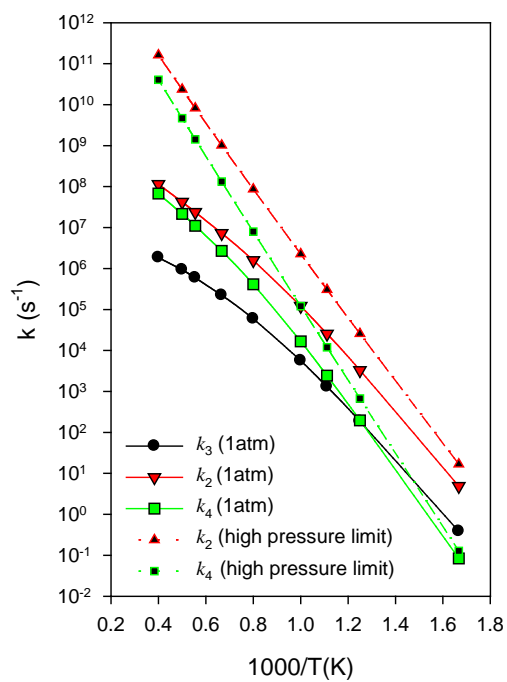


Figure 2

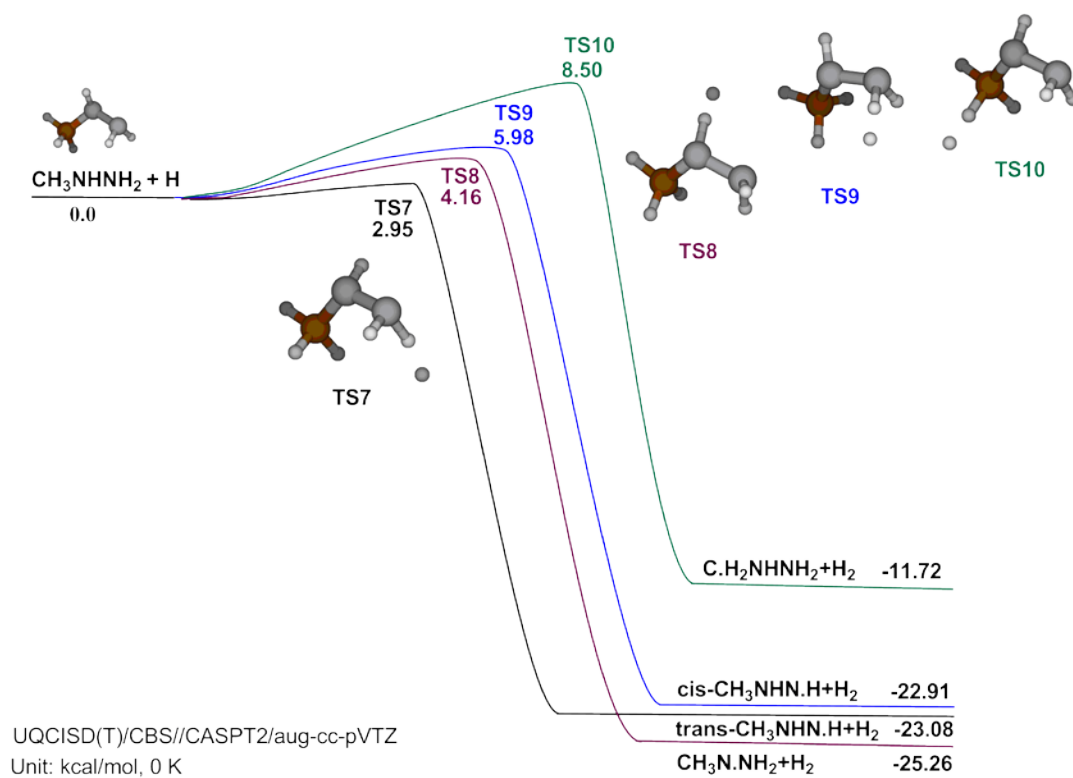


Figure 3

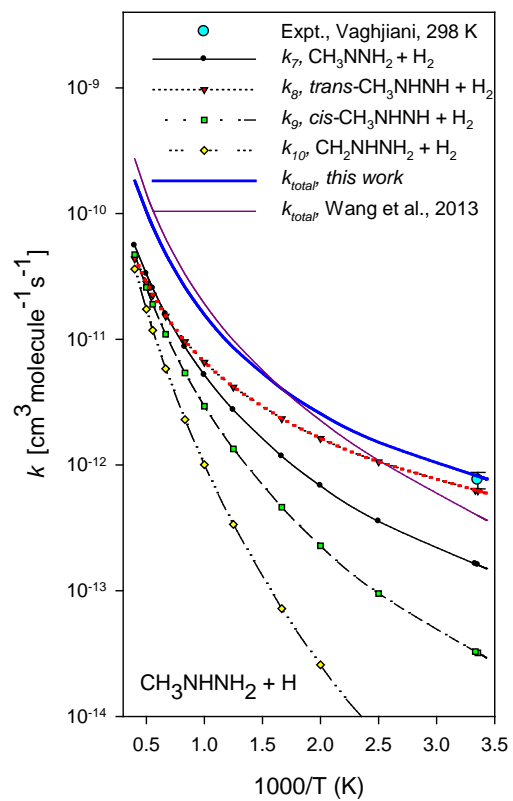


Figure 4

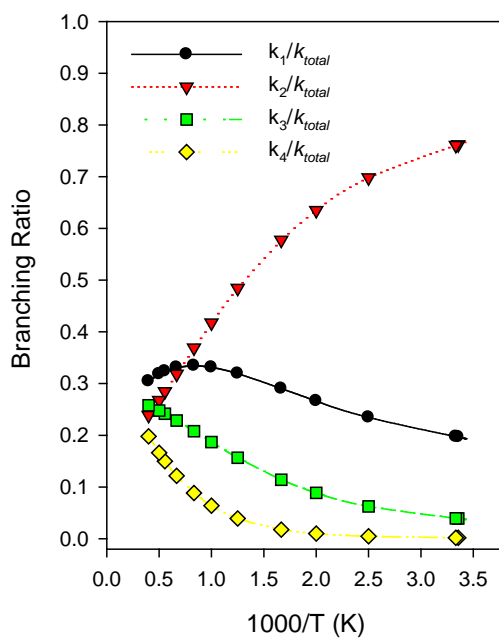


Figure 5

Figure Captions

Figure 1. Potential energy surfaces for $\text{CH}_3\text{N}\cdot\text{H}$ radical decomposition.

Figure 2. Rate coefficients of CH_3NH radical dissociation in the temperature range 600 - 2500K.

Figure 3. Potential energy surfaces for $\text{CH}_3\text{NHH}_2 + \text{H}$ reaction calculated at the UQCISD(T)/cc-pV ∞ Z//CASPT2/aug-cc-pVTZ level.

Figure 4. Theoretical abstraction rate coefficients for $\text{CH}_3\text{NHH}_2 + \text{H}$ reaction, with comparison of experimental data.

Figure 5. Theoretical abstraction branching ratios for $\text{CH}_3\text{NHH}_2 + \text{H}$ reaction as a function of temperature.